

Mutant analyses reveal different functions of *fgfr1* in medaka and zebrafish despite conserved ligand–receptor relationships

Hayato Yokoi^{a,1}, Atsuko Shimada^a, Matthias Carl^b, Shigeo Takashima^{a,2}, Daisuke Kobayashi^a, Takanori Narita^{a,3}, Tomoko Jindo^{a,4}, Tetsuaki Kimura^{a,5}, Tadao Kitagawa^{a,6}, Takahiro Kage^a, Atsushi Sawada^{a,7}, Kiyoshi Naruse^a, Shuichi Asakawa^c, Nobuyoshi Shimizu^c, Hiroshi Mitani^d, Akihiro Shima^{d,8}, Makiko Tsutsumi^e, Hiroshi Hori^e, Joachim Wittbrodt^f, Yumiko Saga^g, Yuji Ishikawa^h, Kazuo Araki^{i,*}, Hiroyuki Takeda^{a,*}

^a Department of Biological Sciences, Graduate School of Science, University of Tokyo, Hongo, Bunkyo-ku, Tokyo 113-0033, Japan

^b Department of Anatomy and Developmental Biology, University College London, Gower Street, London, WC1E 6BT, UK

^c Department of Molecular Biology, Keio University School of Medicine, Shinjuku-ku, Tokyo 160-8582, Japan

^d Department of Integrated Biosciences, Graduate School of Frontier Sciences, University of Tokyo, Kashiwa, Chiba 277-8562, Japan

^e Division of Biological Science, Graduate School of Science, Nagoya University, Furo-cho, Chikusa-ku, Nagoya 464-8602, Japan

^f Developmental Biology Unit, EMBL-Heidelberg, Meyerhofstraße 1, 69012 Heidelberg, Germany

^g Division of Mammalian Development, National Institute of Genetics, Yata, Mishima 411-8540, Japan

^h National Institute of Radiological Sciences, Inage-ku, Chiba, Japan

ⁱ Farming Biology Division, National Research Institute of Aquaculture, Mie 519-0423, Japan

Received for publication 27 October 2006; revised 15 December 2006; accepted 19 December 2006

Available online 23 December 2006

Abstract

Medaka (*Oryzias latipes*) is a small freshwater teleost that provides an excellent developmental genetic model complementary to zebrafish. Our recent mutagenesis screening using medaka identified *headfish* (*hdf*) which is characterized by the absence of trunk and tail structures with nearly normal head including the midbrain–hindbrain boundary (MHB). Positional-candidate cloning revealed that the *hdf* mutation causes a functionally null form of Fgfr1. The *fgfr1^{hdf}* is thus the first *fgf receptor* mutant in fish. Although FGF signaling has been implicated in mesoderm induction, mesoderm is induced normally in the *fgfr1^{hdf}* mutant, but subsequently, mutant embryos fail to maintain the mesoderm, leading to defects in mesoderm derivatives, especially in trunk and tail. Furthermore, we found that morpholino knockdown of medaka *fgf8* resulted in a phenotype identical to the *fgfr1^{hdf}* mutant, suggesting that like its mouse counterpart, Fgf8 is a major ligand for Fgfr1 in medaka early embryogenesis. Intriguingly, Fgf8 and Fgfr1 in zebrafish are also suggested to form a major ligand–receptor pair, but their function is much diverged, as the zebrafish *fgfr1* morphant and zebrafish *fgf8* mutant *acerebellar* (*ace*) only fail to develop the MHB, but develop nearly unaffected trunk and tail. These results provide evidence that teleost fish have evolved divergent functions of Fgf8–Fgfr1 while maintaining the

* Corresponding authors. Kazuo Araki is to be contacted at Farming Biology Division, National Research Institute of Aquaculture, Mie 519-0423, Japan. Fax: +81 596 58 6413. Hiroyuki Takeda, Department of Biological Sciences, Graduate School of Science, University of Tokyo, Hongo, Bunkyo-ku, Tokyo 113-0033, Japan. Fax: +81 3 5841 4993.

E-mail addresses: arakin@affrc.go.jp (K. Araki), htakeda@biol.s.u-tokyo.ac.jp (H. Takeda).

¹ Present address: Institute of Neuroscience, University of Oregon, Eugene, OR 97402, USA.

² Present address: Department of Molecular, Cell and Developmental Biology, University of California, Los Angeles, CA 90095, USA.

³ Present address: Center for Genetic Resources Information, National Institute of Genetics, Yata, Mishima 411-8540, Japan.

⁴ Present address: Nakagawa Initiative Research Unit, RIKEN, Wako, Saitama 351-0198, Japan.

⁵ Present address: Department of Molecular Life Science, Tokai University School of Medicine, Isehara, Kanagawa 259-1193, Japan.

⁶ Present address: Department of Environmental Management, Faculty of Agriculture, Kinki University, Nara 631-8505, Japan.

⁷ Present address: Laboratory for Embryonic Induction, RIKEN Center for Developmental Biology, Chuo-ku, Kobe 650-0047, Japan.

⁸ Present address: Institute for Environmental Sciences, Rokkasho 039-3212, Japan.

ligand–receptor relationships. Comparative analysis using different fish is thus invaluable for shedding light on evolutionary diversification of gene function.

© 2006 Elsevier Inc. All rights reserved.

Keywords: Medaka; Zebrafish; *fgfr1*; Mesoderm; *fgf8*; Evolution; Divergence of gene function

Introduction

Medaka (*Oryzias latipes*) is a model vertebrate of increasing interest in developmental and evolutionary biology (Ishikawa, 2000; Wittbrodt et al., 2002; Naruse et al., 2004). In addition to common shared features with zebrafish, medaka has several advantages i.e. a smaller genome (about 800 Mb, half the size of the zebrafish genome), the existence of highly polymorphic inbred strains and a wide range of growth permissive temperatures. Recently, a large-scale mutagenesis screening was conducted and has delivered a vastly expanded pool of medaka mutant stocks (Furutani-Seiki et al., 2004). As expected from the great evolutionary distance between medaka and zebrafish (more than 110 million years) (Wittbrodt et al., 2002), some medaka mutations appear to have unique phenotypes, demonstrating the utility of multiple teleost genetic models. In our recent mutagenesis screening, we isolated a medaka mutant, *headfish* (*hdf*), showing a severe defect in trunk–tail development, a phenotype that has not yet been identified in zebrafish screening. Analysis reported here revealed that *hdf* mutants have a null mutation in the medaka *fgf receptor 1* gene (*fgfr1*), and this therefore represents the first *fgf-receptor*-related mutant in fish.

The FGF receptor is a cell surface receptor tyrosine kinase that binds FGFs extracellularly and transduces resulting signals into the cytosol (Böttcher and Niehrs, 2005). Among the four *Fgf receptors*, *Fgfr1* is thought to play a critical role in vertebrate early development, particularly in mesoderm formation and neural patterning. In frog and fish embryos, functional analysis of *Fgfr1* has mainly involved injection of RNA molecules encoding a dominant-negative form of FGFR1 (XFD), because no mutant for *Fgfr1* has been available in these animals prior to the present study. However, the phenotype induced by XFD (Amaya et al., 1991, 1993; Griffin et al., 1995; Launay et al., 1996; Carl and Wittbrodt, 1999) is somewhat different from those observed in *Fgfr1*-knockout mice (Deng et al., 1994; Yamaguchi et al., 1994). This is particularly evident for the initial formation of mesoderm which occurs in mice in the absence of FGFR1, but does not occur in fish and frogs in the presence of XFD. This could be due either to a species specificity of FGFR1 function or to the lack of specificity of the XFD (Ueno et al., 1992). Hence, the *fgfr1^{hdf}* mutant enables us to genetically identify the role of *Fgfr1* for the first time in fish development.

Due to promiscuity of FGF receptors and the large number of possible ligands, ligand–receptor relationships are complex in FGF signaling (Zhang et al., 2006), which sometimes hampers molecular dissection of FGF-mediated signaling. Among FGF ligands examined, FGF8 is thought to exert its

function mainly through FGFR1 in mesoderm and neural patterning, as both the *fgf8*- and *Fgfr1*-knockout mice exhibit similar defects during gastrulation (Deng et al., 1994; Yamaguchi et al., 1994; Sun et al., 1999) and in midbrain–hindbrain boundary (MHB) formation (Chi et al., 2003; Trokovic et al., 2003, 2005). Phenotypic similarity between *fgfr1* and *fgf8*-defective embryos was also reported in zebrafish, although their phenotype is much milder and limited to the MHB (Scholpp et al., 2004). These results suggest that ligand–receptor relationships in FGF signaling tend to be conserved during vertebrate evolution despite divergent function. In this study, we first report the positional cloning and phenotypes of the *fgfr1^{hdf}* mutant, which genetically reveals the specific roles of *Fgfr1* during early embryogenesis in fish. Then, we discuss the evolution of Fgf receptor–ligand system by comparing the phenotypes of medaka and zebrafish *fgfr1*- and *fgf8*-defective embryos.

Materials and methods

Medaka strains for ENU mutagenesis and mapping

Two Japanese medaka strains were used in mutagenesis and mapping. The strain used for mutagenesis screening was d-rR strain of a closed colony, derived from the southern Japanese population (Yamamoto, 1953). The strain used for genetic mapping was the inbred strain HNI, derived from the northern population (Hyodo-Taguchi, 1980). Embryos were obtained by natural mating and staged according to morphology as described (Iwamatsu, 1994).

Adult male fish of the d-rR strain were mutagenized with 3 mM *N*-ethyl-*N*-nitrosourea (ENU), as described previously (Ishikawa, 1996; Ishikawa et al., 1999). Mutant screening was performed at the F3 generation according to morphological criteria. The *headfish* (*hdf*) mutant was isolated as a recessive embryonic lethal mutant showing severe abnormalities in the trunk and tail region. The mutant line was maintained as a heterozygous fish in a d-rR genetic background.

Genetic mapping and chromosome walking

The mutant fish of d-rR background were crossed with the HNI, and the F1 hybrids were intercrossed to generate a reference panel for mapping. Genomic DNA extraction from medaka embryos was performed as described in Kimura et al. (2004). The mutant locus was mapped by scoring for recombination with STS markers using the M-marker system as described previously (Kimura et al., 2004). Further detailed mapping was performed using a 633 F2 progeny panel of 1266 meioses. Medaka *spt* was mapped using primers designed based on the EST sequence (primers: AGGACC-TACGTCCACCC and GTGGGTATTGACTCCACTCTGC). Arrayed filters of a medaka bacterial artificial chromosomes (BAC) library (Matsuda et al., 2001) were screened by hybridization using the AlkPhos direct labeling and detection system (Amersham Biosciences). Both ends of the BAC clone were sequenced and converted to STS markers which were then used for typing of the reference panel. The BAC library was screened using the STS marker as a probe.

Morpholino and mRNA injection

Morpholino oligonucleotides (MO) were obtained from GeneTools (Corvallis, OR). A morpholino targeted to the 1st methionine of the medaka *spt* (*tbx16*) gene, MO-*tbx16*: AGCTCTGTGATGGACTGCATTCTTC. Splicing morpholinos targeted to the splice donor site of the medaka *fgfr1* located at the junction of exon 11 and intron 11, and of exon 15 and intron 15, are MO-*fgfr1*SP1: TATCTACTTTCTGTTACCTGTCTGC and MO-*fgfr1*SP2: GGTCGTGGTGT-TTTTACCTTTTAG. Morpholinos targeted to the 1st methionine of the medaka *fgfr1* gene are MO-*fgfr1*M1: ATAGTATTCTTGGCCTCATCAGCAT and MO-*fgfr1*M4: GAACATCAGCTGTGAACATTCACG. A morpholino targeted to the 1st methionine of the medaka *fgf8* gene is MO-*fgf8*: ATAGCTGCATGG-CACGGGTCTCATC. Morpholinos were dissolved in 100 μ l of distilled water at a concentration of 3 mM and stored at -20°C . For injection, the morpholino solutions were diluted to 60–300 μM in final concentration of $1\times$ Yamamoto's solution containing 0.05% phenol red.

To synthesize RNA in vitro, the open reading frame of the medaka *fgfr1* was cloned into the plasmid pCS2+. The plasmid was linearized, and capped sense RNA was synthesized using SP6 mMessage machine kit (Ambion, Austin, TX). The synthesized RNA was purified using the RNeasy purification filter (QIAGEN) and diluted to the concentration of 1 $\mu\text{g}/\mu\text{l}$ and stored at -80°C until use. For injection, RNA solution was diluted to 200–500 ng/ μl in final concentration of $1\times$ Yamamoto's solution containing 0.05% phenol red.

Sample eggs for injection were collected from the abdomen of female fish, 20 min after the mating of male and female fish that had been separated the previous evening. Morpholinos or RNA solutions were injected into the cytoplasm of 1-cell stage embryos. Injected embryos were incubated in the medaka hatching buffer at 28°C .

Bead transplantation

Heparin gel beads (EY Laboratories, Inc.) were washed three times in PBS and in 0.1% BSA (Sigma)/PBS. The beads were incubated with 0.25 mg/ml recombinant mouse FGF8B protein (R&D Systems) or 0.1% BSA/PBS for 2 h at room temperature, and then washed twice with 0.1% BSA/PBS.

For bead transplantation, embryos were dechorionated using hatching enzyme in the medaka balanced salt solution (BSS). Embryos were soaked in the hatching enzyme solution at the morula stage (st. 8–9) and the degraded chorion was removed by st. 11 using a melted round-headed glass needle. Dechorionated embryos were incubated in the medaka BSS. Transplantation was performed on a 1.5% agarose plate filled with medaka BSS. An FGF-soaked or a BSA bead was transplanted into the dorso-lateral part of the blastoderm of the dechorionated embryos using a tungsten needle and a melted round-headed glass needle at the shield stage (around st. 13). Bead transplanted embryos were incubated in BSS until the desired stage and fixed with 4% PFA/0.85 \times PBST overnight for in situ analysis.

Whole-mount in situ hybridization

Embryos were fixed with 4% paraformaldehyde (PFA)/PBST and dehydrated with methanol. After rehydration, samples were treated with proteinase K, then refixed with PFA, followed with PBST washes. They were then treated with hybridization mixture (50% formamide, 5 \times SSC, 50 $\mu\text{g}/\text{ml}$ heparin, 100 $\mu\text{g}/\text{ml}$ calf thymus DNA, 10 $\mu\text{g}/\text{ml}$ tRNA, 0.1% Tween-20) for 1 h and incubated with DIG-labeled RNA probe at 65°C overnight. After washing with a series of SSC and blocking with 2% fetal calf serum (FCS), the samples were incubated with alkaline phosphate (AP)-conjugated anti-DIG Fab fragments (1:8000) at 4°C overnight. Detection was performed with BM-purple (Roche). Samples after staining were washed with PBS containing 1% Tween-20 several times for each overnight to reduce the background staining.

Phylogenetic analysis

Protein sequences were obtained from GenBank. Species and GenBank accession numbers are shown in the figure. The sequences were aligned using CLUSTAL W program (Thompson et al., 1994) and phylogenetic trees

were constructed using the neighbor-joining method in the DDBJ website (<http://www.ddbj.nig.ac.jp/search/clustalw-j.html>).

Results

Morphological and gene expression characteristics of headfish mutant

The *headfish* (*hdf*) mutant was isolated in our recent screening of ENU-induced mutants affecting the embryonic development and organogenesis in medaka. The *hdf* is a recessive lethal mutant showing drastic phenotypes; it lacks most of the posterior structures at the hatching stage (9 days post-fertilization), whereas the head structure appears almost normal (Figs. 1A–D). At the early segmentation stage, no or few somites are formed in the mutant (Figs. 1E, F), while anterior structures are relatively normal (Figs. 1G, H). As judged by *myod* and *paraxial protocadherin* (*papc*) expression (markers for the muscle and presomitic mesoderm, respectively), the paraxial mesoderm which gives rise to the somite does not differentiate normally (Figs. 1K–N). In contrast, most of the axial mesoderm develops in the *hdf* mutant (Figs. 1E, F), but is abnormal in shape, as evidenced by punctuated expression of *ntl* (*no tail*, also called *brachyury*), a marker for notochord (Figs. 1O, P). These defects in mesodermal differentiation can be ascribed to a failure of maintenance of the tailbud which gives rise to nearly all mesodermal derivatives; the expression of *spt* (*spadetail*, also called *tbx16*), a tailbud marker, is almost gone in the mutant (Figs. 1Q, R). Consequently, the tail does not elongate properly and the resulting body length of the mutant embryo is much shorter than wild type (Figs. 1I, J). *ntl* is also a marker for the earliest mesoderm induced at the late blastula stage, and we found the normal levels of *ntl* expression in the blastoderm margin of all embryos obtained from heterozygous parents (no morphological phenotype is detectable at this stage), suggesting that mesoderm is normally induced in the *hdf* mutant (Fig. 1S). Similarly, the initial dorsoventral specification normally takes place in the mutant, as indicated by normal *chordin* expression (Fig. 1T).

headfish encodes medaka *fgfr1*

To identify the gene responsible for *hdf*, we employed a positional-candidate cloning strategy. The *hdf* locus was genetically mapped to the medaka linkage group (LG) 9 by bulked segregant analysis with the M-marker system (Kimura et al., 2004). We identified an EST marker, OLb0402d, that is tightly linked to the *hdf* locus (one recombination in 1266 meioses) (Fig. 2A). Chromosome walking using BAC clones was then conducted to narrow down the responsible region. In parallel, mapping of candidate genes and comparative syntenic analysis with the genome of *Fugu rubripes* identified *spt* and *fgfr1* in the responsive region (0 and 1 recombination in 852 meioses, respectively).

Morpholino-knockdown of *spt* resulted in an enlarged tailbud with normal somites, which is comparable to the phenotype of the zebrafish *spt* mutant (Griffin et al., 1998) (data

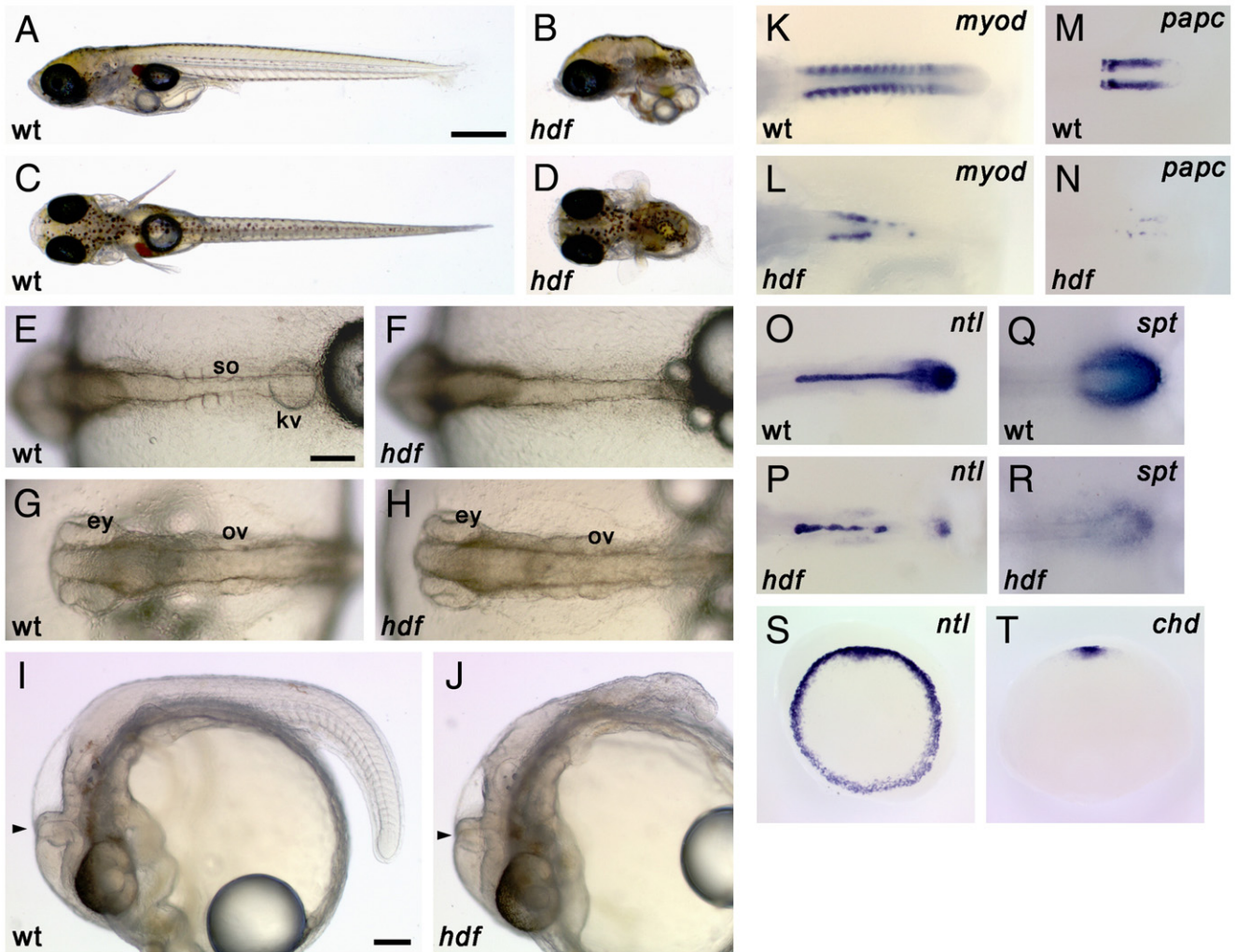


Fig. 1. Morphology and gene expression in *headfish* mutant embryos. (A–J) External morphology. Wild-type (A, C) and *hdf* mutant (B, D) embryos at hatching stage (st. 39). Lateral view (A, B) and dorsal view (C, D). Mutant embryos lack most of the posterior part of the body. On the other hand, head development appears normal. Wild-type (E, G) and *hdf* mutant (F, H) embryos at 4-somite stage (st. 20). Dorsal view of the tail (E, F) and head (G, H). Mutant embryos have a midline structure but fail to form somites. Lateral view of wild-type (I) and *hdf* mutant (J) embryos at 30-somite stage (st. 28). *hdf* mutant embryos show agenesis of the posterior structures but have a morphologically normal head, including the eyes, ventricles and MHB (arrowhead). ey, eye; kv, Kupffer's vesicle; ov, otic vesicle; so, somite. Scale bars: (A) 500 μ m; (E) 100 μ m; (I) 100 μ m. (K–T) Gene expression patterns. Wild-type (K, M, O, Q) and mutant (L, N, P, R) embryos during early segmentation stages. (K, L) The expression of *myod*, a somite differentiation marker, is observed in each somite in a wild-type embryo, in a bilateral regular stripe pattern (K), whereas it is severely reduced in the mutant embryos (L). (M, N) The expression of *papc*, a presomitic mesoderm marker, is lost and only faint expression is observed in the mutant (N). (O, P) The expression of *ntl*, a pan-mesodermal marker. *ntl* expression is detected in the notochord and tailbud in wild-type (O), but is down-regulated in tailbud and exhibits an interrupted pattern in midline of the mutant embryos (P). (Q, R) The expression of *spt*, a marker for the tailbud. While *spt* is expressed in the tailbud of the wild-type embryo (Q), it is considerably weaker in the mutant embryo (R). (S, T) Early gastrula stage. Animal-pole views are shown. *ntl* is expressed uniformly in the blastoderm margin of all sibling embryos obtained from a heterozygous mating (S) and *chordin*, a dorsal mesodermal marker is detected in the dorsal region of all sibling embryos (T). Each genotype is indicated as *wt*, *wild-type* and *hdf*, *headfish*.

not shown). Significantly, the injection of morpholinos against *fgfr1* was found to phenocopy the *hdf* mutant; we obtained the somite-less phenotype with normal head structures at a greater than 95% frequency with the morpholinos designed at two different exon–intron boundaries (MO-*fgfr1*SP1 and MO-*fgfr1*SP2) (Figs. 2D–G). We then determined the full-length cDNA and the genomic organization of medaka *fgfr1* and finally identified a single nucleotide alteration G-to-C in exon 6, resulting in an amino acid substitution, tryptophan to cysteine (W181C), in the extracellular Ig-like domain II (IGII) (Fig. 2B). This tryptophan is conserved among all FGFRs isolated,

including insects and mammals (Fig. 2C). Therefore, it must be crucial for the function of FGFR1. But there is no functional annotation for this tryptophan thus far. The *hdf* mutant will help define the role of this tryptophan.

The somite-less phenotype of the *hdf* mutant was rescued at the segmentation stage by injection of RNA encoding wild-type *Fgfr1* (Figs. 2H–J), whereas the mutant *fgfr1* RNA of the mutant (W181C) did not rescue the defect (data not shown). Moreover, wild-type embryos showed no obvious phenotype when injected by wild-type or mutant RNA (data not shown), suggesting that the mutation W181C is a loss-of-function type.

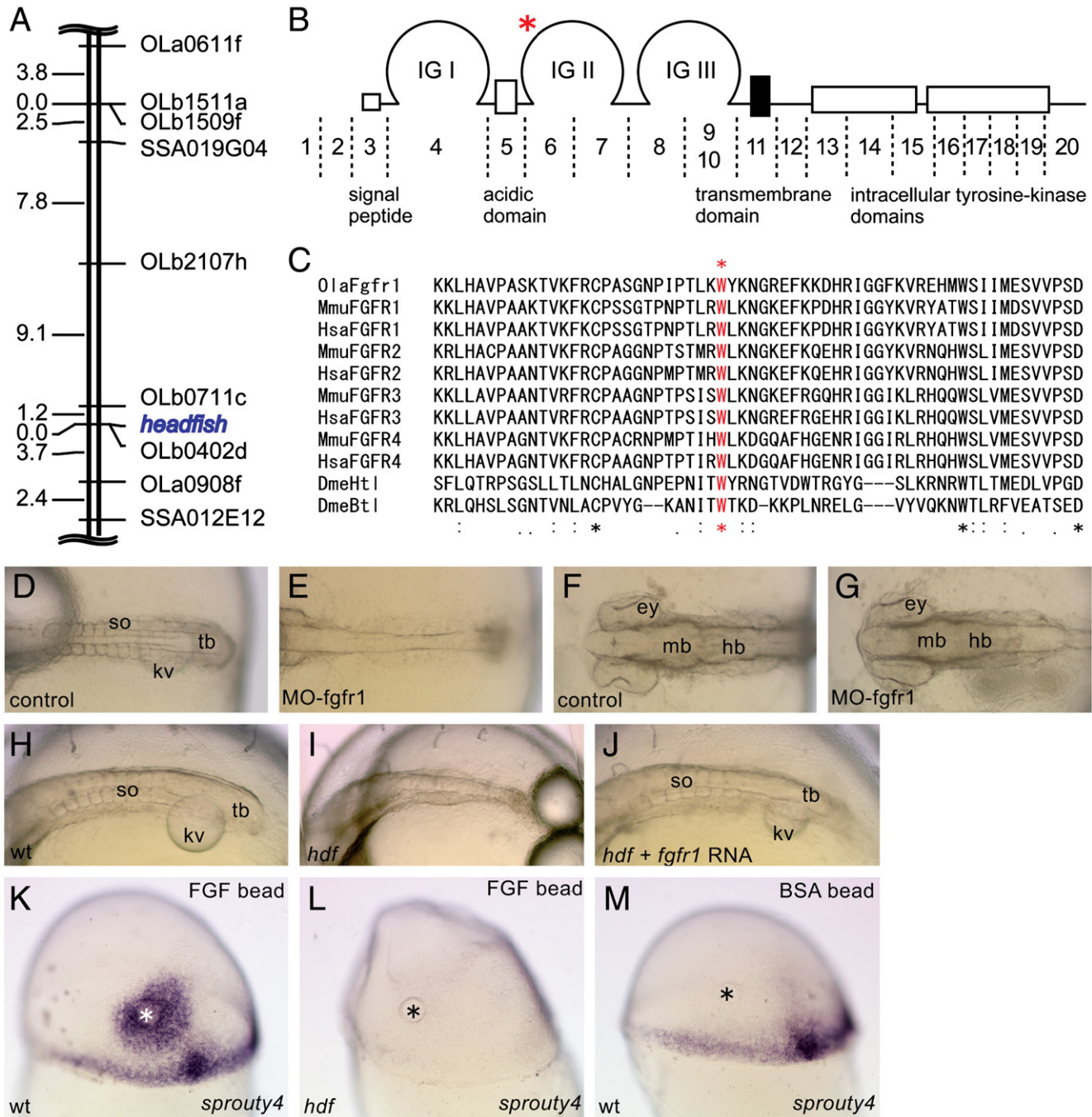


Fig. 2. Genetic mapping and identification of the *headfish* mutation. (A) The *hdf* locus is roughly mapped in the middle of medaka LG9, near the EST marker OLa0402d. (B) Structure of FGFR1 and its corresponding exons. Medaka *fgfr1* consists of at least 20 exons. A G-to-C point mutation was found in exon 6, indicated by a red asterisk. The mutation causes an amino acid substitution W181C in the second immunoglobulin (IG) domain. (C) The mutated tryptophan residue is conserved among all of the FGFRs from *Drosophila* to human, indicating its essential role for the FGFR function. (D–G) Morpholino knock-down of *fgfr1*. Dorsal views of the trunk (D, E) and head (F, G) regions of control (D, F) and morphant (E, G) embryos are shown. Note that MO injection phenocopies *hdf* mutants. Anterior to the left. (H–J) Rescue of the mutant phenotype by injection of RNA encoding wild-type Fgfr1. Oblique dorsal views of the trunk region of control (H), *hdf* mutant (I) and RNA-injected *hdf* mutant (J) are shown. Note that the injected *hdf* mutant forms somites (J). Anterior to the left. (K–M) Responsiveness to exogenous FGFs. Mid-gastrula embryos transplanted with FGF8-beads on the dorsal side were stained with *sprouty4* probe. Lateral views of wild-type (K), *hdf* mutant (L) and control wild-type (M) embryos are shown. Animal pole to the top. The control embryo was transplanted with a BSA-soaked bead (M). In addition to endogenous expression in the marginal and dorsal mesoderm, *sprouty4* expression is induced around the FGF8-beads (K), whereas the FGF8-beads fail to induce *sprouty4* in the *hdf* mutant (L).

Finally, we confirmed reduced responsiveness to FGFs in the mutant by showing that FGF8-soaked-beads transplanted into gastrula-stage mutant embryos fail to induce the expression of *sprouty4*, one of the known downstream targets of FGF

signaling (Fürthauer et al., 2001) (Figs. 2K–M). Based on these results, we conclude that disruption of *fgfr1* causes *hdf* and that the amino acid substitution of W181C is responsible for Fgfr1 dysfunction.

The expression of *fgfr1* and *sprouty4* during wild-type and mutant development

Fig. 3 shows the normal expression of *fgfr1* during medaka embryogenesis. Ubiquitous maternal expression of *fgfr1* was detected in the early cleavage-stage embryo (4-cell, Fig. 3A). Ubiquitous expression including the blastoderm margin is maintained until early gastrula stage, during which the expression gradually increases in the dorsal half (Figs. 3B, C). At the early gastrula stage (st. 15), elevated expression is detected in the dorsal margin, presumptive anterior neural region, and the underlying hypoblast (Fig. 3D, histological sections not shown). However, as gastrulation proceeds, these elevated anterior expression domains gradually decrease as expression is up-regulated in the trunk–tail region of the neuroectoderm and mesoderm including the tailbud (Figs. 3E, H). At this stage, *sprouty4* is strongly activated as a stripe in the middle part of the presumptive neuroectoderm (probably the future midbrain–hindbrain boundary) as well as in the dorsal marginal mesoderm fated to become the notochord and tailbud. This activation of *sprouty4*, however, is not detected in the mutant embryo, which is consistent with the *fgfr1^{hdf}* phenotype (Figs. 3F, G).

During the bud stage to early segmentation stages, *fgfr1* is broadly expressed in the trunk region, somites and presomitic mesoderm (Figs. 3I, K), while *sprouty4* exhibits restricted expression in the anterior tip of the telencephalon, MHB, rhombomere 4 and tailbud (Figs. 3M, O). Among these *sprouty4* expression domains, expression in the telencephalon is less affected in the mutant (Figs. 3N, P), while the expression in other regions is reduced or lost. These results indicate that *sprouty4* expression is highly dependent on Fgfr1-mediated signaling, except in the telencephalon, and thus, Fgfr1 is likely to be the primary mediator for FGF signaling in the blastoderm margin and tailbud.

Expression of anterior neural markers in wild-type and *fgfr1^{hdf}* embryos

FGF signaling has been implicated in forebrain patterning and MHB formation, but *fgfr1^{hdf}* embryos develop morphologically normal head structures. We thus examined the expression of region-specific neural markers in wild-type and *fgfr1^{hdf}* mutant embryos at the bud (st. 18) to 9-somite (st. 21) stages. The markers used were *bfl* for the telencephalon (data not shown), *pax6* for the forebrain and hindbrain, *pax2* for MHB and *krox20* for rhombomeres 3 and 5 (Fig. 4) (Kage et al., 2004). These region-specific markers are almost normally expressed in *fgfr1^{hdf}* mutant embryos, except for *krox20*. Expression of *krox20* in rhombomere 5 tends to be frequently missing or reduced in *fgfr1^{hdf}* mutants until the 6-somite stage (st. 21) (Figs. 4D, E). Expression of *krox20*, however, is recovered by the 9-somite stage (Fig. 4F), suggesting that Fgfr1 function is initially required but later compensated by other Fgf receptors expressed in this region. Furthermore, the most ventral region of the anterior head normally develops as indicated by *hedgehog* expression (Figs. 4J, M). These results

indicate that Fgfr1-mediated signaling is largely dispensable for development of most anterior head structures.

Fgf8 is a major functional ligand of *Fgfr1* in medaka

FGF8 is a well-characterized FGF ligand and functions in various tissues of vertebrate development. In zebrafish, Fgf8 has been suggested to act mainly through Fgfr1 because of the phenotypic similarity between the *fgf8^{ace}* mutant and *fgfr1* morphant (Scholpp et al., 2004). The zebrafish phenotype, however, is evident mainly in the MHB, which forms normally in *fgfr1^{hdf}* mutants. To examine whether this ligand–receptor relationship is maintained in medaka, we analyzed the expression and function of medaka *fgf8*. For this, we have isolated medaka *fgf8* using medaka EST (http://medaka.lab.nig.ac.jp/est_index.html) and genome information (UTGB: <http://dolphin.lab.nig.ac.jp/medaka/>). Medaka *fgf8* is expressed in the anterior tip of the telencephalon, MHB, hindbrain and tailbud (Figs. 5A, B), which is similar to that of zebrafish *fgf8* and mouse *fgf8*, except that, unlike zebrafish *fgf8*, the somitic mesoderm does not express *fgf8* in medaka. These expression patterns are largely unaffected in the *fgfr1^{hdf}* mutants, except in the tailbud where the expression is reduced and dispersed (Figs. 5C, D).

We then examined the function of medaka *fgf8* by knocking down *fgf8* gene function with MOs. Surprisingly, the phenotype of *fgf8* morphants is nearly identical to that of *fgfr1^{hdf}* mutants (Figs. 5E–H); MO-injected embryos exhibit the somite-less phenotype. The morphant embryos develop morphologically normal head including MHB, which is also similar to the *fgfr1^{hdf}* mutants. The expression of *krox20* and *pax2* is analyzed in the morphant head, in order to examine the rhombomere patterning defect observed in the *fgfr1^{hdf}* mutant. The expression of *krox20* is only detected in r3 and lost in r5 at st. 18, and the expression in r5 is recovered by st. 20 (Figs. 5I–L). This defect-recovery phenotype is quite similar to that in the *fgfr1^{hdf}* mutant (Figs. 4A–F). Same as the *fgfr1^{hdf}* mutant, the expression of *pax2* in MHB is not affected in the *fgf8* morphant (Figs. 5M–P). These results suggest that Fgfr1 is also a primary transducer of Fgf8 signaling in medaka during embryogenesis, but that the function of the Fgfr1 and Fgf8 pair is different in different teleost lineages.

Discussion

Disruption of *fgfr1* causes the headfish phenotype

The recessive lethal mutant *hdf* was found to be the first *fgf-receptor*-related mutant in fish. The mutation we identified causes a substitution of the 181st amino acid, tryptophan, to cysteine in the extracellular Ig-like domain II (IGII) of Fgfr1. The IGII domain is known to be essential for interacting with ligands and with heparan sulfate proteoglycan, a co-factor for FGFRs (Böttcher and Niehrs, 2005). Although there have been no functional studies on this mutated tryptophan, the *fgfr1^{hdf}* mutant has uncovered its critical role in the function of FGFR1; this residue is not suggested to interact directly with FGF ligand nor heparin (Pellegrini et al., 2000; Schlessinger et al., 2000),

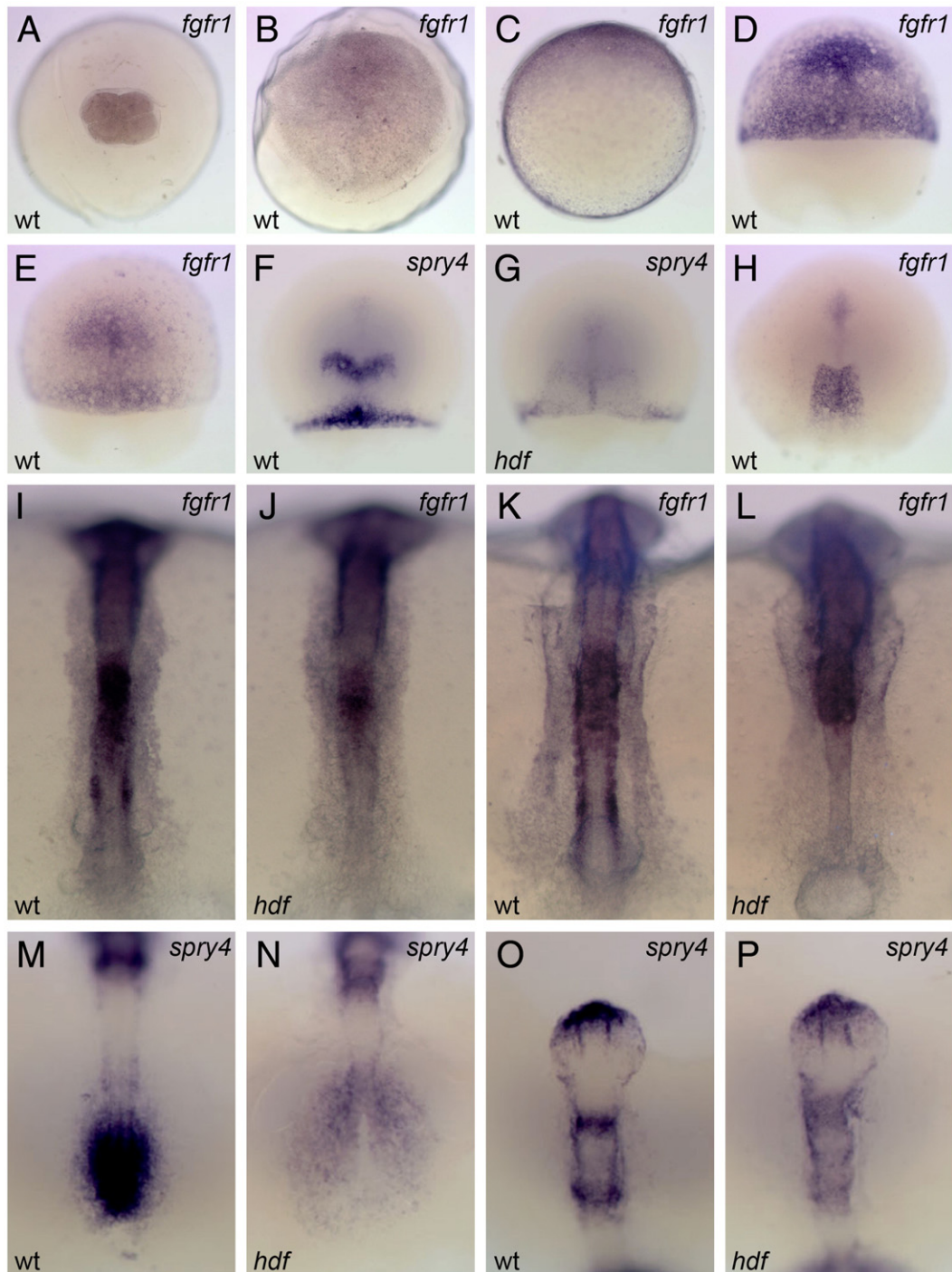


Fig. 3. Embryonic expression of medaka *fgfr1* and its down-stream target, *sprouty4*. Probes used are on the top right corner. wt, wild-type and *hdf, fgfr1^{hdf}* mutant embryos. Animal-pole views (A–B) and dorsal views (E–P; animal-pole or anterior to the top) are shown. Maternal expression of medaka *fgfr1* is detected ubiquitously at st. 4 (4-cell) (A). At st. 13 (early gastrula), *fgfr1* is expressed ubiquitously with higher levels on the dorsal side (to the top; C). During gastrulation, *fgfr1* is expressed in the presumptive head region with the continued expression in the margin (D, st. 15; E, st. 15+). The expression of *sprouty4* is observed in the presumptive MHB and dorsal margin in a part of the sibling embryos (F), but in some siblings this expression is undetectable (G). At the end of gastrulation, *fgfr1* is expressed in the trunk region (H). At the bud stage (I) and the early segmentation stage (K), *fgfr1* is expressed in the trunk, paraxial mesoderm, somite and presomitic mesoderm. In the neural tube, weak ubiquitous expression with high levels in the hindbrain is observed in the wild-type embryo (I, K). In the mutant, *fgfr1* expression is lost in the paraxial mesoderm, somites and presomitic mesoderm, due to a lack of these tissues, whereas the expression in the anterior portion remains unchanged (J, L). At these stages, *sprouty4* is expressed in the tailbud (M), the anterior tip of telencephalon, MHB and r4 (O). The *sprouty4* expression is lost in the tailbud and reduced in the mutant (N, P), except for the telencephalon.

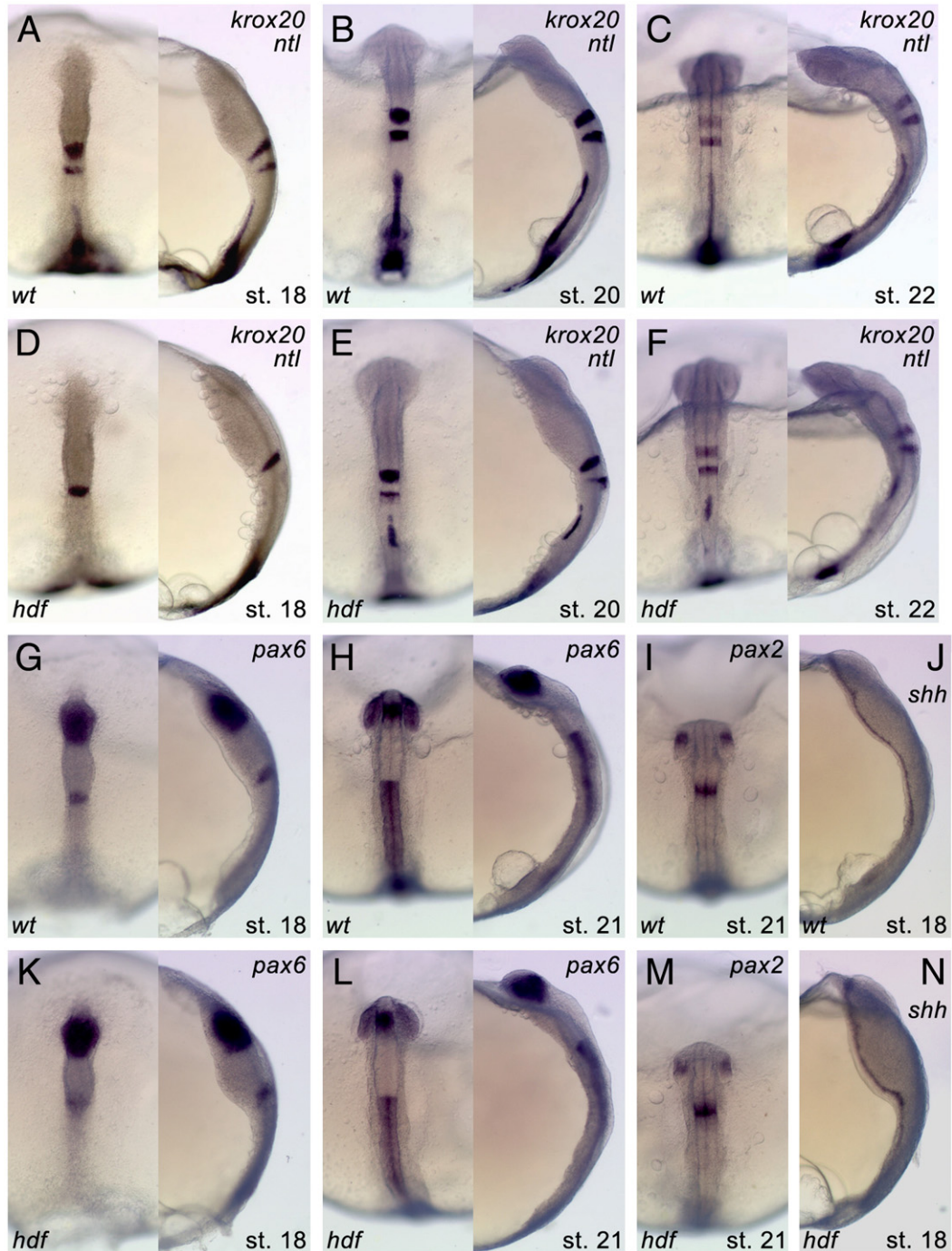


Fig. 4. Activity of *fgfr1* is transiently required for rhombomere patterning. Dorsal view and lateral view of wild-type (A–C, G–J) and *fgfr1*^{hdf} (D–F, K–N) embryos. At st. 18, *krox20* expression in the r5 is lost in the mutant, whereas the expression in r3 is not affected (A, D). The expression in r5 is restoring at st. 20 in the mutant (B, E), and is recovered at st. 22 (C, F). The expression of *pax6* in forebrain and hindbrain is normal in the mutant (G, H, K, L). The expression of *pax2* in MHB (I, M) and *shh* in prechordal plate and floor plate (J, N) are not affected in the mutant.

and is probably essential for formation of a ternary structure. This idea is further supported by the fact that this amino acid is conserved among all types of FGFRs isolated from nematode to vertebrates.

Four lines of evidence suggest that the *fgfr1*^{hdf} allele is likely to cause a simple loss-of-function of *fgfr1* activities: (1) *fgfr1*^{hdf} is a recessive mutant and heterozygous fish show no phenotype.

(2) The *fgfr1*^{hdf} mutant phenotype is rescued by the injection of wild-type *fgfr1* mRNA. (3) Injection of mRNA encoding the *fgfr1*^{hdf} mutant has no effect on wild-type embryos. (4) Gene knock-down of *fgfr1* using several different MO-*fgfr1* constructs phenocopies the *fgfr1*^{hdf} mutant phenotype. Further structural and functional analysis will shed light on the precise function of this tryptophan residue in FGF receptors.

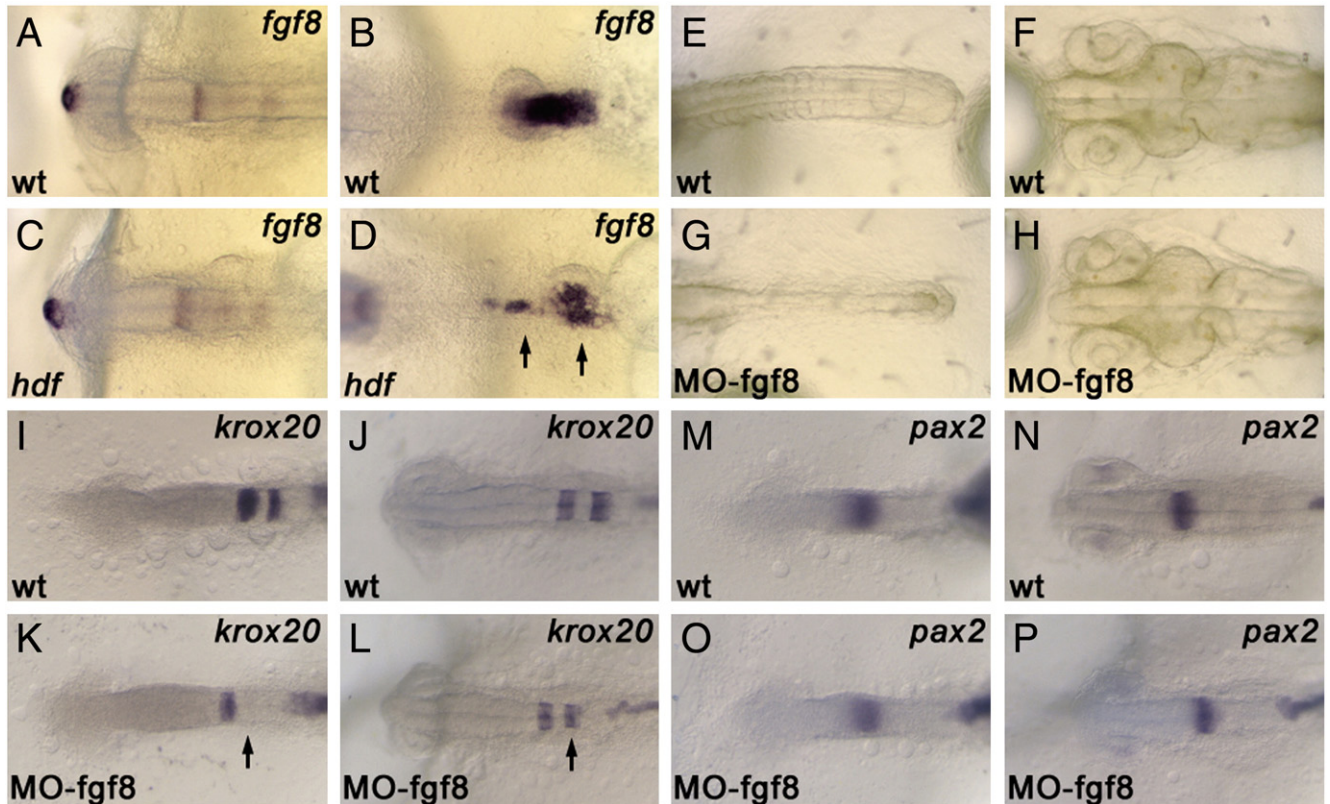


Fig. 5. The expression of *fgf8* and the phenotype of *fgf8*-morphant. Medaka *fgf8* is expressed in the anterior tip of the forebrain, MHB, hindbrain and tailbud (A, B). The expression of *fgf8* is largely unaffected in the *fgfr1^{hdf}* mutant, except for the expression in tailbud (C, D; arrows). Injection of *fgf8* morpholino causes somite-less phenotype, phenocopying the *fgfr1^{hdf}* mutant phenotype (E, G). Same as *fgfr1^{hdf}*, morphology of the brain including MHB is normal in the *fgf8* morphant (H). The expression of *krox20* and *ntl* in wild-type (I, J) and *fgf8* morphant (K, L). In the morphant, the expression of *krox20* in r5 is lost at st. 18, and is recovered at st. 20 (K, L; arrows). The expression of *pax2* and *ntl* in wild-type (M, N) and *fgf8* morphant (O, P). The expression of *pax2* in MHB is not affected in the morphant.

Is *Fgfr1*-mediated signaling dispensable for mesoderm induction?

In fish and frog, the functional analysis of *Fgfr1* has been mainly performed by the injection of mRNA encoding a dominant negative form of FGFR1 (XFD). The results of these experiments demonstrated that the blocking of FGF signaling in early *Xenopus* and zebrafish embryos inhibits mesoderm induction, leading to truncation of the anterior–posterior axis (Amaya et al., 1991, 1993; Griffin et al., 1995; Launay et al., 1996; Carl and Wittbrodt, 1999). The receptor mediating the FGF signal, however, has not been clear because XFD interacts with all of FGFRs and thus interferes with all the signals mediated by FGFRs (Ueno et al., 1992). Indeed, in the *Fgfr1*-mutant mouse, initial mesoderm formation occurs normally (Deng et al., 1994; Yamaguchi et al., 1994), suggesting that FGF signaling mediated by receptors other than FGFR1 could conceivably compensate and participate in this process. The analysis of *fgfr1^{hdf}* mutants supports this interpretation. Together with the phenotype of *Fgfr1* knockout mice, our results demonstrate that FGFR1-mediated signaling is rather required for subsequent mesoderm patterning and maintenance in vertebrate embryos. Since the presence of maternal products may attenuate the phenotype of a zygotic mutant of fish (Gritsman et al., 1999; Mintzer et al., 2001), the definitive

answer awaits production of maternal–zygotic medaka mutants for *fgfr1*. In preliminary experiments, we have found that the expression of *ntl* persists at the blastula stage in maternal–zygotic *fgfr1^{hdf}* mutants, suggesting that *Fgfr1*-mediated signaling is dispensable for mesoderm induction in fish. Detailed phenotypes of maternal–zygotic *fgfr1^{hdf}* mutant including defective cell movement will be described elsewhere (Shimada et al., unpublished results).

Fgfr1-mediated signaling in neural patterning

A number of previous studies have demonstrated that FGFs secreted from the anterior neural ridge, MHB (isthmus region) and rhombomere 4 are implicated in patterning of the telencephalon, midbrain and hindbrain (Crossley et al., 1996; Shimamura and Rubenstein, 1997; Shanmugalingam et al., 2000; Shinya et al., 2001; Maves et al., 2002; Walshe et al., 2002; Sato et al., 2004). In the *fgfr1^{hdf}* mutant, however, the expression patterns of regional neural markers and *sprouty4* in the anterior head seem largely unaffected or recovered, suggesting that other FGFRs redundantly function during anterior neural patterning. Indeed, we and other groups have observed that medaka *fgf receptors 2–4* are differentially expressed in the anterior head with some overlapping domains (Carl and Wittbrodt, 1999; data not shown). The maternally

supplied Fgfr1 may not be involved in this relatively late patterning event, because transplantation of FGF8-beads revealed that *fgfr1^{hdf}* mutants of mid-gastrula stage have already lost their ability to respond to exogenous FGFs (Figs. 2K–N). Hence maternal Fgfr1, if any, loses its major effects by mid-gastrulation.

Divergent function and conserved ligand–receptor pair of fish Fgf8–Fgfr1

The receptor specificity of FGF ligands has been intensely examined in cell culture systems, and recent in vitro analysis demonstrates that various types of FGFRs can transduce FGF8 signal (Zhang et al., 2006). On the other hand, *Fgfr* mutants provide key information on ligand–receptor relationships in vivo, and FGFR1 was thought to be a major transducer for FGF8 signal in mouse early development. Indeed, *Fgfr1* mutant mice exhibit a nearly identical phenotype to *fgf8* mutants; they do not form proper mesoderm (Deng et al., 1994; Yamaguchi et al., 1994; Sun et al., 1999). In contrast, the phenotype of the zebrafish *fgf8^{ace}* mutant is mild and restricted to the MHB (Reifers et al., 1998). Interestingly, the zebrafish *fgfr1* morphant exhibits the similar phenotype; it fails to form the MHB with only mildly affected somitogenesis (Scholpp et al., 2004), suggesting that the ligand–receptor pair, FGF8–FGFR1, is conserved in zebrafish.

The conserved ligand–receptor pair between mouse and zebrafish could be coincidence or a result of co-evolution. In the present study, we tested these possibilities by comparing the phenotypes of *fgfr1^{hdf}* mutants with that of *fgf8* morphants. Morpholino knock-down of medaka *fgf8* resulted in almost the

same phenotype to that observed in the medaka *fgfr1^{hdf}* mutant, including normal MHB formation. Furthermore, our phylogenetic analysis confirms that the medaka Fgfr1 and Fgf8 examined here are the ortholog of the zebrafish Fgfr1 and Fgf8, respectively (Fig. 6). It is worth noting that the milder phenotypes in zebrafish could be a result of incomplete inhibition of each gene function. However, this can not fully account for the phenotypic differences in the MHB and rhombomere 4 between the two fishes; the MHB is specifically defective in zebrafish mutants or morphants, while rhombomere 4 in medaka counterparts. Taken together, we conclude that in spite of the functional difference, the ligand–receptor pair of FGF8–FGFR1 is maintained between the two fish lineages. Hence, after the divergence of medaka and zebrafish, which is estimated around 110–160 MYA (million years ago) (Wittbrodt et al., 2002), they differently evolved the functions of Fgf8–Fgfr1 signal and/or its degree of redundancy with other signals, while maintaining the ligand–receptor relationship. Indeed, it was recently found that *fgf24* redundantly functions with *fgf8* to promote posterior development in zebrafish; inactivation of both *fgf24* and *fgf8* in zebrafish causes a phenotype similar to medaka *fgf8* morphants (Draper et al., 2003). The conserved functional pair of Fgf8–Fgfr1 found in two fish and mouse suggests the presence of unknown developmental constraint that promotes co-evolution of this signaling system. Thorough studies using various species will provide further insights into evolutionary diversification of the Fgf ligand–receptor system.

In conclusion, we have isolated the first *fgfr1* mutant in fish and have conducted phenotypic analyses of the mutant. Considering the advantages of fish experimental systems, the *fgfr1^{hdf}* mutant is a valuable model with which to genetically

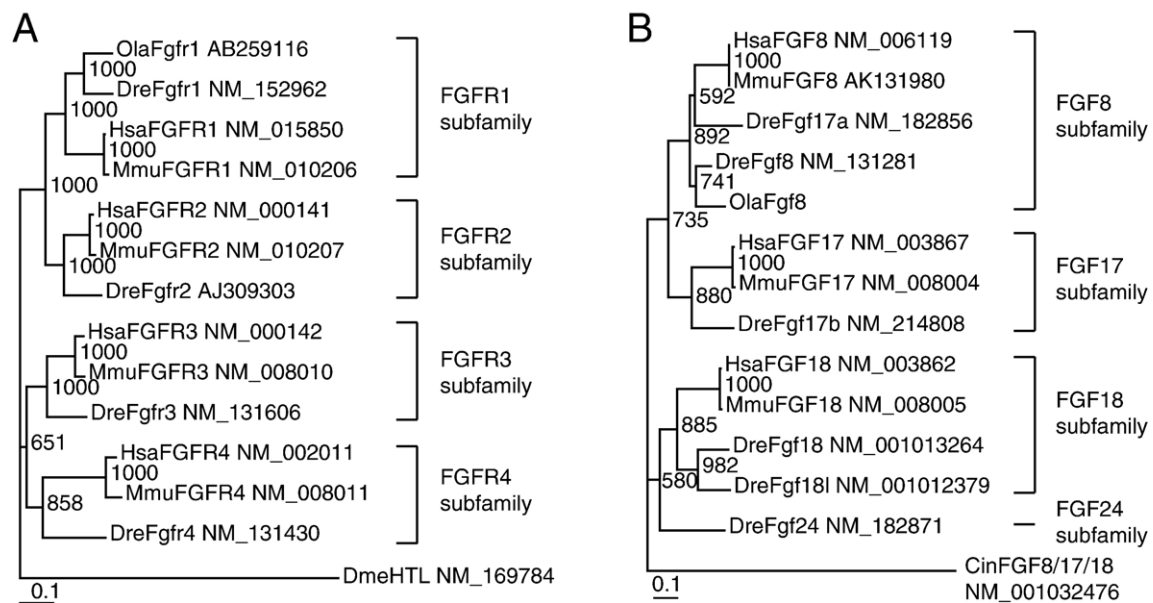


Fig. 6. Phylogenetic trees of FGFR1 and FGF8. Trees are written by the neighbor-joining method using amino acid sequences. Sequences are obtained from GenBank. The numbers on the branches are the bootstrap values for the group in a thousand runs. The marker length corresponds to a 10% sequence difference. (A) A NJ tree of FGFR. Medaka Fgfr1 analyzed here is the ortholog of zebrafish Fgfr1 (NM_152962). *Drosophila* Heartless (HTL: NM_169784) was used as an outgroup. (B) A NJ tree of FGF8/17/18 subfamily. Medaka Fgf8 analyzed here is the ortholog of zebrafish Fgf8 (NM_131281). *Ciona intestinalis* FGF8/17/18 (NM_001032476) was used as an outgroup. Cin: ascidian, *Ciona intestinalis*; Dme: fruit fly, *Drosophila melanogaster*; Dre: zebrafish, *Danio rerio*; Hsa: human, *Homo sapiens*; Mmu: mouse, *Mus musculus*; Ola: medaka, *Oryzias latipes*.

analyze the precise role of Fgfr1-mediated signaling in various aspects of development, growth and differentiation. Comparative analysis with *fgf8* morphant further revealed a conserved receptor–ligand relationship with divergent functions of Fgfr1 during vertebrate evolution. We showed the significance of the use of two different teleost fish species to gain new insights into the function of genes, and their evolutionary diversification.

Accession numbers

Genomic and cDNA sequences are deposited to the DDBJ/EMBL/GenBank. The accession numbers are as follows: medaka *fgfr1* gene, AB259115; medaka *fgfr1* IIIc VT+ isoform cDNA, AB259116; medaka *fgfr1* IIIc VT-isoform cDNA, AB259117; medaka *fgfr1* IIIb VT+ isoform cDNA, AB259118; medaka *fgfr1* IIIb VT-isoform cDNA, AB259119; and medaka *fgfr1* gene *headfish* mutation, AB259120.

Acknowledgments

We are grateful to Ms Miki Sugimoto, Aki Ito-Igarashi, Kaeko Nakaguchi, Satoko Minami, Yeon-Hwa Park, Yasuko Ozawa, Kazuyo Ohki and Tomomi Obata for excellent fish care and experimental assistance. We are also grateful to Prof. John H. Postlethwait for critical reading of the manuscript. We thank Dr Minoru Tanaka (National Institute for Basic Biology) for providing the myod plasmid, and Drs Keiji Inohaya and Shigeaki Yasumasu (Sophia Univ.) for the *krox20* plasmid. Our mutant screening was carried out mainly at the National Institute of Genetics (NIG), supported by NIG Cooperative Research Program (2002–2006). This work was supported in part by Grants-in-Aid for Scientific Research Priority Area Genome Science and the Organized Research Combination System from the Ministry of Education, Culture, Sports, Science and Technology of Japan and a Bio-Design Project of the Ministry of Agriculture, Forestry and Fisheries of Japan. HY was supported by Research Fellowships of the Japan Society for the Promotion of Science for Young Scientists.

The authors would like to dedicate this paper to late Prof. Kenjiro Ozato of Nagoya University who passed away Sept 21, 2006.

References

- Amaya, E., Musci, T.J., Kirschner, M.W., 1991. Expression of a dominant negative mutant of the FGF receptor disrupts mesoderm formation in *Xenopus* embryos. *Cell* 66, 257–270.
- Amaya, E., Stein, P.A., Musci, T.J., Kirschner, M.W., 1993. FGF signalling in the early specification of mesoderm in *Xenopus*. *Development* 118, 477–487.
- Böttcher, R.T., Niehrs, C., 2005. Fibroblast growth factor signaling during early vertebrate development. *Endocr. Rev.* 26, 63–77.
- Carl, M., Wittbrodt, J., 1999. Graded interference with FGF signalling reveals its dorsoventral asymmetry at the mid–hindbrain boundary. *Development* 126, 5659–5667.
- Chi, C.L., Martinez, S., Wurst, W., Martin, G.R., 2003. The isthmic organizer signal FGF8 is required for cell survival in the prospective midbrain and cerebellum. *Development* 130, 2633–2644.
- Crossley, P.H., Martinez, S., Martin, G.R., 1996. Midbrain development induced by FGF8 in the chick embryo. *Nature* 380, 66–68.
- Deng, C.X., Wynshaw-Boris, A., Shen, M.M., Daugherty, C., Ornitz, D.M., Leder, P., 1994. Murine FGFR-1 is required for early postimplantation growth and axial organization. *Genes Dev.* 8, 3045–3057.
- Draper, B.W., Stock, D.W., Kimmel, C.B., 2003. Zebrafish *fgf24* functions with *fgf8* to promote posterior mesodermal development. *Development* 130, 4639–4654.
- Fürthauer, M., Reifers, F., Brand, M., Thisse, B., Thisse, C., 2001. *sprouty4* acts in vivo as a feedback-induced antagonist of FGF signaling in zebrafish. *Development* 128, 2175–2186.
- Furutani-Seiki, M., Sasado, T., Morinaga, C., Suwa, H., Niwa, K., Yoda, H., Deguchi, T., Hirose, Y., Yasuoka, A., Henrich, T., Watanabe, T., Iwanami, N., Kitagawa, D., Saito, K., Asaka, S., Osakada, M., Kunitatsu, S., Momoi, A., Elmasri, H., Winkler, C., Ramialison, M., Loosli, F., Quiring, R., Carl, M., Grabher, C., Winkler, S., Del Bene, F., Shinomiya, A., Kota, Y., Yamanaka, T., Okamoto, Y., Takahashi, K., Todo, T., Abe, K., Takahama, Y., Tanaka, M., Mitani, H., Katada, T., Nishina, H., Nakajima, N., Wittbrodt, J., Kondoh, H., 2004. A systematic genome-wide screen for mutations affecting organogenesis in medaka, *Oryzias latipes*. *Mech. Dev.* 121, 647–658.
- Griffin, K., Patient, R., Holder, N., 1995. Analysis of FGF function in normal and no tail zebrafish embryos reveals separate mechanisms for formation of the trunk and the tail. *Development* 121, 2983–2994.
- Griffin, K.J., Amacher, S.L., Kimmel, C.B., Kimmel, D., 1998. Molecular identification of *spadetail*: regulation of zebrafish trunk and tail mesoderm formation by T-box genes. *Development* 125, 3379–3388.
- Gritsman, K., Zhang, J., Cheng, S., Heckscher, E., Talbot, W.S., Schier, A.F., 1999. The EGF–CFC protein one-eyed pinhead is essential for nodal signaling. *Cell* 97, 121–132.
- Hyodo-Taguchi, Y., 1980. Establishment of inbred strains of the teleost, *Oryzias latipes*. *Zool. Mag. (Tokyo)* 89, 283–301.
- Ishikawa, Y., 1996. A recessive lethal mutation, *tb*, that bends the midbrain region of the neural tube in the early embryo of the medaka. *Neurosci. Res.* 24, 313–317.
- Ishikawa, Y., 2000. Medaka fish as a model system for vertebrate developmental genetics. *BioEssays* 22, 487–495.
- Ishikawa, Y., Hyodo-Taguchi, Y., Aoki, K., Yasuda, T., Matsumoto, A., Sasanuma, M., 1999. Induction of mutations by ENU in the medaka germline. *Fish Biol. J. Medaka* 10, 27–29.
- Iwamatsu, T., 1994. Stages of normal development in the medaka *Oryzias latipes*. *Zool. Sci.* 11, 825–839.
- Kage, T., Takeda, H., Yasuda, T., Maruyama, K., Yamamoto, N., Yoshimoto, M., Araki, K., Inohaya, K., Okamoto, H., Yasumasu, S., Watanabe, K., Ito, H., Ishikawa, Y., 2004. Morphogenesis and regionalization of the medaka embryonic brain. *J. Comp. Neurol.* 476, 219–239.
- Kimura, T., Jindo, T., Narita, T., Naruse, K., Kobayashi, D., Shin, I.T., Kitagawa, T., Sakaguchi, T., Mitani, H., Shima, A., Kohara, Y., Takeda, H., 2004. Large-scale isolation of ESTs from medaka embryos and its application to medaka developmental genetics. *Mech. Dev.* 121, 915–932.
- Launay, C., Fromentoux, V., Shi, D.L., Boucaut, J.C., 1996. A truncated FGF receptor blocks neural induction by endogenous *Xenopus* inducers. *Development* 122, 869–880.
- Matsuda, M., Kawato, N., Asakawa, S., Shimizu, N., Nagahama, Y., Hamaguchi, S., Sakaizumi, M., Hori, H., 2001. Construction of a BAC library derived from the inbred Hd-rR strain of the teleost fish, *Oryzias latipes*. *Genes Genet. Syst.* 76, 61–63.
- Maves, L., Jackman, W., Kimmel, C.B., 2002. FGF3 and FGF8 mediate a rhombomere 4 signaling activity in the zebrafish hindbrain. *Development* 129, 3825–3837.
- Mintzer, K.A., Lee, M.A., Runke, G., Trout, J., Whitman, M., Mullins, M.C., 2001. *Lost-a-fin* encodes a type I BMP receptor, Alk8, acting maternally and zygotically in dorsoventral pattern formation. *Development* 128, 859–869.
- Naruse, K., Hori, H., Shimizu, N., Kohara, Y., Takeda, H., 2004. Medaka genomics: a bridge between mutant phenotype and gene function. *Mech. Dev.* 121, 619–628.
- Pellegrini, L., Burke, D.F., von Delft, F., Mulloy, B., Blundell, T.L., 2000. Crystal structure of fibroblast growth factor receptor ectodomain bound to ligand and heparin. *Nature* 407, 1029–1034.
- Reifers, F., Bohli, H., Walsh, E.C., Crossley, P.H., Stainier, D.Y., Brand, M.,

1998. Fgf8 is mutated in zebrafish *acerebellar* (*ace*) mutants and is required for maintenance of midbrain–hindbrain boundary development and somitogenesis. *Development* 125, 2381–2395.
- Sato, T., Joyner, A.L., Nakamura, H., 2004. How does Fgf signaling from the isthmus organizer induce midbrain and cerebellum development? *Dev. Growth Differ.* 46, 487–494.
- Schlessinger, J., Plotnikov, A.N., Ibrahimi, O.A., Eliseenkova, A.V., Yeh, B.K., Yayon, A., Linhardt, R.J., Mohammadi, M., 2000. Crystal structure of a ternary FGF–FGFR–heparin complex reveals a dual role for heparin in FGFR binding and dimerization. *Mol. Cell* 6, 743–750.
- Scholpp, S., Groth, C., Lohs, C., Lardelli, M., Brand, M., 2004. Zebrafish *fgfr1* is a member of the *fgf8* synexpression group and is required for *fgf8* signalling at the midbrain–hindbrain boundary. *Dev. Genes Evol.* 214, 285–295.
- Shanmugalingam, S., Houart, C., Picker, A., Reifers, F., Macdonald, R., Barth, A., Griffin, K., Brand, M., Wilson, S.W., 2000. *Ace*/Fgf8 is required for forebrain commissure formation and patterning of the telencephalon. *Development* 127, 2549–2561.
- Shimamura, K., Rubenstein, J.L., 1997. Inductive interactions direct early regionalization of the mouse forebrain. *Development* 124, 2709–2718.
- Shinya, M., Koshida, S., Sawada, A., Kuroiwa, A., Takeda, H., 2001. Fgf signalling through MAPK cascade is required for development of the subpallial telencephalon in zebrafish embryos. *Development* 128, 4153–4164.
- Sun, X., Meyers, E.N., Lewandoski, M., Martin, G.R., 1999. Targeted disruption of Fgf8 causes failure of cell migration in the gastrulating mouse embryo. *Genes Dev.* 13, 1834–1846.
- Thompson, J.D., Higgins, D.G., Gibson, T.J., 1994. CLUSTAL W: improving the sensitivity of progressive multiple sequence alignment through sequence weighting, position-specific gap penalties and weight matrix choice. *Nucleic Acids Res.* 22, 4673–4680.
- Trokovic, R., Trokovic, N., Hernesniemi, S., Pirvola, U., Vogt Weisenhorn, D.M., Rossant, J., McMahon, A.P., Wurst, W., Partanen, J., 2003. FGFR1 is independently required in both developing mid- and hindbrain for sustained response to isthmus signals. *EMBO J.* 22, 1811–1823.
- Trokovic, R., Jukkola, T., Saarimaki, J., Peltopuro, P., Naserke, T., Weisenhorn, D.M., Trokovic, N., Wurst, W., Partanen, J., 2005. Fgfr1-dependent boundary cells between developing mid- and hindbrain. *Dev. Biol.* 278, 428–439.
- Ueno, H., Gunn, M., Dell, K., Tseng Jr., A., Williams, L., 1992. A truncated form of fibroblast growth factor receptor 1 inhibits signal transduction by multiple types of fibroblast growth factor receptor. *J. Biol. Chem.* 267, 1470–1476.
- Walshe, J., Maroon, H., McGonnell, I.M., Dickson, C., Mason, I., 2002. Establishment of hindbrain segmental identity requires signaling by FGF3 and FGF8. *Curr. Biol.* 12, 1117–1123.
- Wittbrodt, J., Shima, A., Schartl, M., 2002. Medaka—A model organism from the far East. *Nat. Rev., Genet.* 3, 53–64.
- Yamaguchi, T.P., Harpal, K., Henkemeyer, M., Rossant, J., 1994. *fgfr-1* is required for embryonic growth and mesodermal patterning during mouse gastrulation. *Genes Dev.* 8, 3032–3044.
- Yamamoto, T., 1953. Artificially induced sex-reversal in genotypic males of the medaka (*Oryzias latipes*). *J. Exp. Zool.* 123, 571–594.
- Zhang, X., Ibrahimi, O.A., Olsen, S.K., Umemori, H., Mohammadi, M., Ornitz, D.M., 2006. Receptor specificity of the fibroblast growth factor family. The complete mammalian FGF family. *J. Biol. Chem.* 281, 15694–15700.